DRUG DESIGN

STRUCTURE- AND LIGAND-BASED APPROACHES

Edited by

Kenneth M. Merz, Jr.
Dagmar Ringe
Charles H. Reynolds

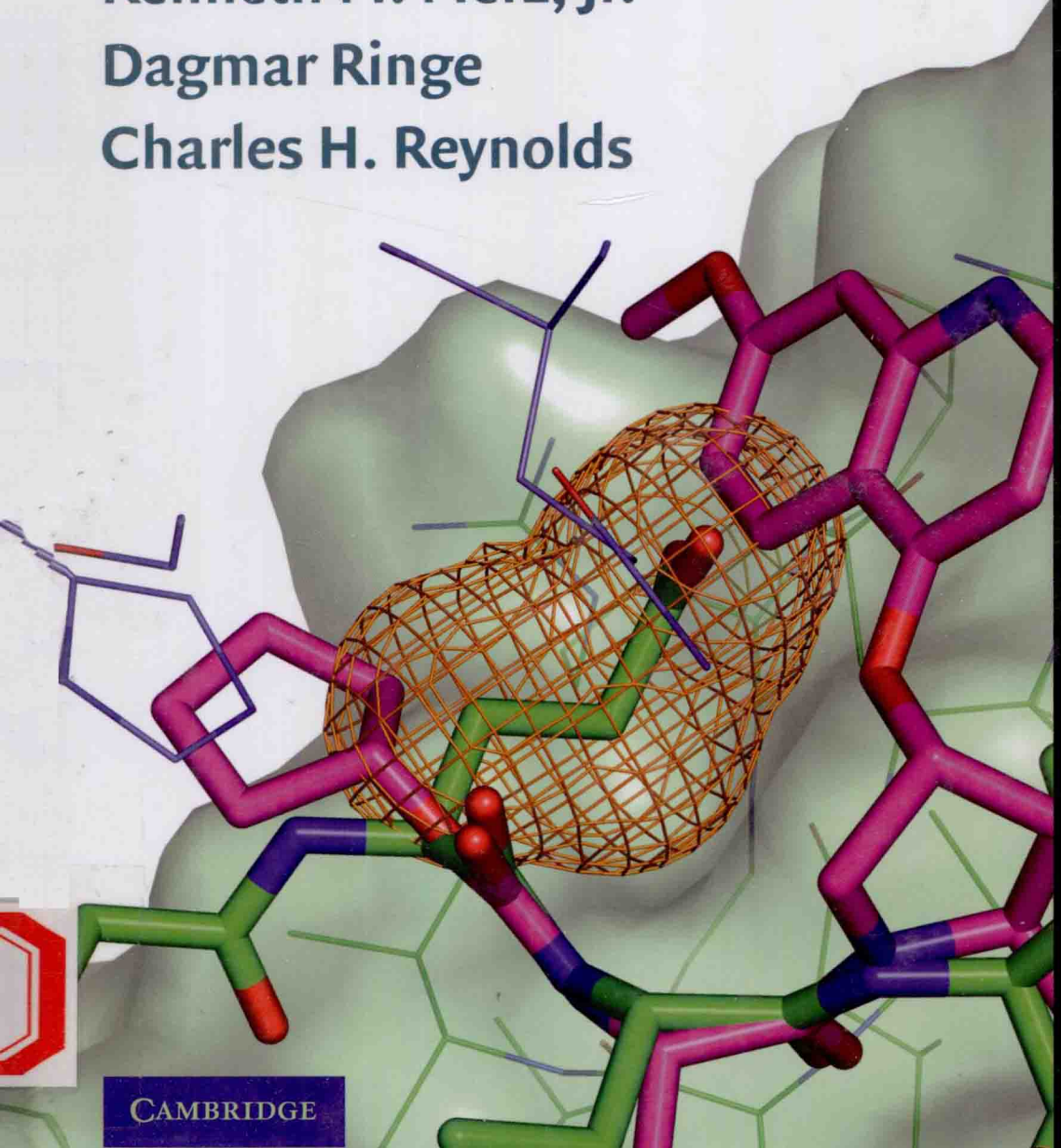

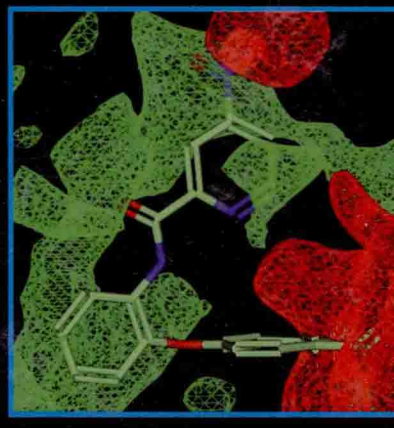

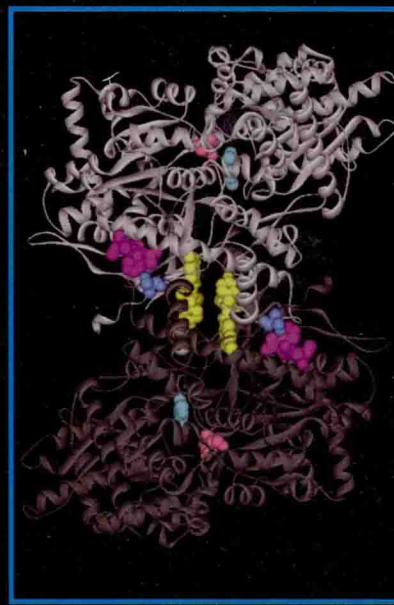

CAMBRIDGE

Drug Design

STRUCTURE- AND LIGAND-BASED APPROACHES

Edited by

Kenneth M. Merz, Jr.
University of Florida, Gainesville

Dagmar Ringe
Brandeis University, Waltham, Massachusetts

Charles H. Reynolds
Johnson & Johnson Pharmaceutical Research and Development,
Spring House, Pennsylvania

CAMBRIDGE
UNIVERSITY PRESS

CAMBRIDGE UNIVERSITY PRESS
Cambridge, New York, Melbourne, Madrid, Cape Town, Singapore,
São Paulo, Delhi, Dubai, Tokyo

Cambridge University Press
32 Avenue of the Americas, New York, NY 10013-2473, USA

www.cambridge.org
Information on this title: www.cambridge.org/9780521887236

First published 2010

Printed in China by Everbest

A catalog record for this publication is available from the British Library.

Library of Congress Cataloging in Publication data

Drug design : structure- and ligand-based approaches / edited by Kenneth M. Merz,
Dagmar Ringe, Charles H. Reynolds.
p. ; cm.
Includes bibliographical references and index.
ISBN 978-0-521-88723-6 (hardback)
1. Drugs – Design. 2. Drugs – Structure-activity relationships. I. Merz, Kenneth M., 1959–
II. Ringe, Dagmar. III. Reynolds, Charles H., 1957– IV. Title.
[DNLM: 1. Drug Design. 2. Ligands. 3. Structure-Activity Relationship.
QV 744 D79327 2010]
RS420.D793 2010
615′.19–dc22 2009051613

ISBN 978-0-521-88723-6 Hardback

Contributors

Frank U. Axe
Axe Consulting Services
Sutter Creek, California

Scott P. Brown
Department of Structural Biology
Abbott Laboratories
Abbott Park, Illinois

Stephen K. Burley
SGX Pharmaceuticals
San Diego, California

Peter J. Connolly
Vertex Pharmaceuticals Inc.
Cambridge, Massachusetts

Qiaolin Deng
Department of Molecular Systems
Merck Research Laboratories
Merck & Co. Inc.
Rahway, New Jersey

Fangyu Ding
Department of Chemistry
Center for Structural Biology
Stony Brook University
Stony Brook, New York

Steven L. Dixon
Schrodinger, Inc.
New York, New York

Arthur M. Doweyko
Research and Development
Computer-Assisted Drug Design
Bristol-Myers Squibb
Princeton, New Jersey

William J. Egan
Novartis Institutes for BioMedical Research
Cambridge, Massachusetts

Martha S. Head
Computational and Structural Chemistry
GlaxoSmithKline Pharmaceuticals
Collegeville, Pennsylvania

Gavin Hirst
SGX Pharmaceuticals
San Diego, California

M. Katharine Holloway
Molecular Systems
Merck Research Laboratories
West Point, Pennsylvania

William L. Jorgensen
Department of Chemistry
Yale University
New Haven, Connecticut

Christopher A. Lepre
Vertex Pharmaceuticals Inc.
Cambridge, Massachusetts

Nigel J. Liverton
Medicinal Chemistry
Merck Research Laboratories
West Point, Pennsylvania

Kenneth M. Merz, Jr.
Department of Chemistry and
Quantum Theory Project
University of Florida
Gainesville, Florida

David L. Mobley
Department of Chemistry
University of New Orleans
New Orleans, Louisiana

Jonathan M. Moore
Vertex Pharmaceuticals Inc.
Cambridge, Massachusetts

Andrew S. Murkin
Department of Biochemistry
Albert Einstein College of Medicine
Bronx, New York

Gregory A. Petsko
Department of Chemistry
Rosenstiel Basic Medical Sciences Research Center
Brandeis University
Waltham, Massachusetts

Siegfried Reich
SGX Pharmaceuticals
San Diego, California

Charles H. Reynolds
Johnson & Johnson Pharmaceutical Research and Development, LLC
Spring House, Pennsylvania

Dagmar Ringe
Department of Chemistry
Rosenstiel Basic Medical Sciences Research Center
Brandeis University
Waltham, Massachusetts

Vern L. Schramm
Department of Biochemistry
Albert Einstein College of Medicine
Bronx, New York

Michael R. Shirts
Department of Chemical Engineering
University of Virginia
Charlottesville, Virginia

Carlos Simmerling
Department of Chemistry
Center for Structural Biology
Stony Brook University
Stony Brook, New York

Paul Sprengeler
SGX Pharmaceuticals
San Diego, California

Alexander Tropsha
Laboratory for Molecular Modeling and
Carolina Center for Exploratory Cheminformatics Research
School of Pharmacy
University of North Carolina at Chapel Hill
Chapel Hill, North Carolina

Preface

Our goal in producing this book is to provide a broad overview of the most important approaches used in protein- and ligand-structure-based drug design. Beyond this we aim to illustrate how these approaches are currently being applied in drug discovery efforts. We hope this book will be a useful resource to practitioners in the field, as well as a good introduction for researchers or students who are new to the field. We believe it provides a snapshot of the most important trends and capabilities in the application of modeling and structural data in drug discovery.

Since the 1990s the role of structure and modeling in drug discovery has grown enormously. There have been remarkable scientific advances in both the experimental and computational fields that are the underpinnings of modern drug design. For example, x-ray capabilities have improved to the point that protein structures are now routinely available for a wide range of protein targets. One only need look at the exponential growth of the Protein Databank (RCSB) for evidence. Tremendous strides have been made in all aspects of protein structure determination, including crystallization, data acquisition, and structure refinement. Modeling has made similar gains. Recent years have brought more realistic force fields, new and more robust free-energy methods, computational models for absorption/distribution/metabolism/excretion (ADME)-toxicity, faster and better docking algorithms, automated 3D pharmacophore detection and searching, and very-large-scale quantum calculations. When coupled with the inexorable increase in computer power, new and improved computational methods allow us to incorporate modeling into the drug discovery process in ways that were not possible just a short time ago.

In addition to improvements in methods, academic and industrial groups have gained significant experience in the application of these approaches to drug discovery problems. Protein structures, docking, pharmacophore searches, and the like have all become a staple of drug discovery and are almost universally applied by large and small pharma companies. A recent example of a new approach that is gaining wider acceptance is fragment-based drug design. The goal of fragment-based design is to build up drug candidates from small low-affinity, but high-information-content, hit structures. As such, fragment-based design relies critically on structural, computational, and biophysical methods to identify, characterize, and elaborate small low-affinity ligands.

The book is divided into three broad categories: structural biology, computational chemistry, and drug discovery applications. Each section contains chapters authored by acknowledged experts in the field. Although no book of reasonable size can be completely comprehensive, we have attempted to address the most significant topics in each category, as well as some areas we see as emergent. We are fortunate to have an introductory chapter from Professor William Jorgensen that sets the tone for the book.

The structural biology section begins with a comprehensive review of the strengths and weaknesses of x-ray crystallography. This is the logical starting point for most protein-structure-based design programs, as crystallography is certainly the most common approach for obtaining the three-dimensional structures of therapeutically important proteins. This section also includes two chapters on fragment-based drug design, including one devoted to the important role nuclear magnetic resonance has played in this new approach.

The computational chemistry section covers a range of modeling techniques, including free-energy methods, dynamics, docking and scoring, pharmacophore modeling, quantitative structure/activity relationships, computational ADME, and quantum methods. Each topic was selected either because it is a commonly employed tool in drug discovery (e.g., docking and scoring) or because it is seen as an emerging technology that may have an increasing role in the future (e.g., linear-scaling quantum calculations). Taken together, these chapters provide a fairly comprehensive overview of the computational approaches being used in drug discovery today.

The final section on applications in drug discovery provides a few concrete examples of using the methods outlined in the first two sections for specific drug discovery programs. This is the ultimate validation of any experimental or computational approach, at least with regard to drug discovery. These examples from six diverse protein targets are useful to the expert as examples of best practices and to the novice as examples of what can be done. An overview of G-protein-coupled receptor (GPCR) modeling and

structure is of keen current interest given that this class has historically been a rich source of drugs, and it has recently seen a major advance in access to experimental structures. This bodes well for the future application of structure-based design to GPCR targets.

Finally, we must thank all the authors who generously agreed to participate in this project for their efforts and patience. Without them, of course, there would be no book. We have been particularly fortunate to enlist such a talented group of authors.

Contents

PART III: APPLICATIONS TO DRUG DISCOVERY

Progress and issues for computationally guided lead discovery and optimization

William L. Jorgensen

INTRODUCTION

Since the late 1980s there have been striking advances, fueled by large increases in both industrial and NIH-funded academic research, that have revolutionized drug discovery. This period has seen the introduction of high-throughput screening (HTS), combinatorial chemistry, PC farms, Linux, SciFinder, structure-based design, virtual screening by docking, free-energy methods, absorption/distribution/metabolism/excretion (ADME) software, bioinformatics, routine biomolecular structure determination, structures for ion channels, G-protein-coupled receptors (GPCRs) and ribosomes, structure/activity relationships (SAR) obtained from nuclear magnetic resonance (SAR by NMR), fragment-based design, gene knockouts, proteomics, small interfering RNA (siRNA), and human genome sequences. The result is a much-accelerated progression from identification of biomolecular target to lead compound to clinical candidate. However, a serious concern is that the dramatic increase in drug discovery abilities and expenditures has not been paralleled by an increase in FDA approvals of new molecular entities.[1] High demands for drug safety, broader and longer clinical trials, too much HTS, too little natural products research, and effective generic drugs for many once-pressing afflictions have all been suggested as contributors.[2–4] Numerous corporate mergers and acquisitions may have also had adverse effects on productivity through distractions of reorganization and integration. Nevertheless, one should consider what the success would have been in the absence of the striking technical advances. Certainly, progress with some critical and challenging target classes such as kinases would have been greatly diminished, and the adverse impact on many cancer patients would have been profound. Indeed, further gains in the treatment and prevention of human diseases must require even more emphasis and commitment to fundamental research. As in other discovery enterprises, the answer is to drill deeper.

The topic of this volume focuses on one of the areas in drug discovery that has seen major transformation and progress: structure- and ligand-based design. The design typically features small molecules that bind to a biomolecular target and inhibit its function. The distinction stems from whether a three-dimensional structure of the target is available and used in the design process. Structure-based design can be carried out with nothing more than the target structure and graphics tools for building ligands in the proposed binding site. However, additional insights provided by evaluation of the molecular energetics for the binding process are central to most current structure-based design activities. Ligand-based design does not require a target structure but rather stems from analysis of structure/activity data for compounds that have been tested in an assay for the biological function of the target. One seeks patterns in the assay results to suggest potential modifications of the compounds to yield enhanced activity. The upside is that a target structure is not required; the downside is that substantial activity data are needed. My research group has focused on the development and application of improved computational methodology for structure-based design. Some of the experiences and issues that have been addressed are summarized in the following.

LEAD GENERATION

Both lead generation and lead optimization may be pursued through joint computational and experimental studies. As summarized in Figure 1.1, our approach has evolved to feature two pathways for lead generation, de novo design with the ligand-growing program BOMB (Biochemical and Organic Model Builder)[5] and virtual screening using the docking program GLIDE.[6] Fragment-based design, which involves the docking and linking together of multiple small molecules in a binding site, is another popular alternative.[7,8] Desirable compounds resulting from de novo design normally have to be synthesized, whereas compounds from virtual screening of commercial catalogs are typically purchased. In both cases, it is preferable to begin with a high-resolution crystal structure for a complex of the target protein with a ligand; though the ligand is removed, it is advisable to start from a complex rather than an apo structure, which may have side chains repositioned to fill partially the binding site. An extreme example occurs with HIV-1 reverse transcriptase (HIV-RT) for which the allosteric binding site for nonnucleoside inhibitors (NNRTIs) is fully collapsed in apo structures.[9]

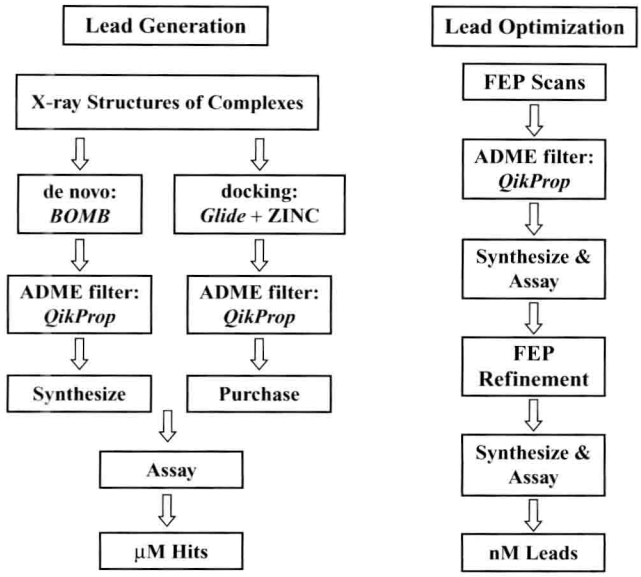

Figure 1.1. Schematic outline for structure-based drug lead discovery and optimization.

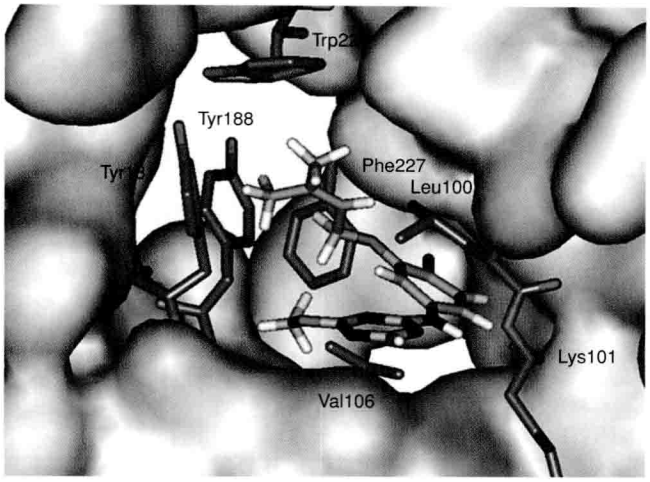

Figure 1.2. An inhibitor built using BOMB in the NNRTI binding site of HIV-RT.

De Novo design with BOMB

BOMB is used to construct complete analogs by adding 0–4 substituents to a core that has been placed in a binding site. A thorough conformational search is performed for each analog, and the position, orientation, and dihedral angles for the analog are optimized using the OPLS-AA force field for the protein and OPLS/CM1A for the analog.[10] The resultant conformer for each analog with the lowest energy is evaluated with a dockinglike scoring function to predict activity. The core may be as simple as, for example, ammonia or benzene, or it may represent a polycyclic framework of a lead series. For the example in Figure 1.2, ammonia was the original core, and it was positioned to form a hydrogen bond with the carbonyl group of Lys101. A library of molecules is then often built using a "template" that has been envisioned by the user to be complementary to the binding site and often to also be amenable to straightforward synthesis. For Figure 1.2, the template was Het-NH-34Ph-U, where Het represents a monocyclic heterocycle, 34Ph is a 3- or 4-substituted phenyl group, and U is an unsaturated hydrophobic group. The template specifies the components that constitute the desired molecules and the topology by which they are linked together.

BOMB includes a library of approximately 700 possible substituents, with code numbers from 1 to about 700, including most common monocyclic and bicyclic heterocycles and about 50 common U groups such as allyl, propargyl, phenyl, phenoxy, and benzyl derivatives. They are provided as groupings by the code numbers or the user can create a custom grouping with desired code numbers. The groupings correspond to template components such as Het, 5Het (just 5-membered ring heterocycles), 6Het, biHet, U, oPhX, mPhX, pPhX, mOPhX, pSPhX, OR, NR, SR, and C = OX. The program then builds all molecules that correspond to the template. In the example, if there were 50 Het and 20 U options, the program would build the 1,000 Het-NH-3-Ph-U and 1,000 Het-NH-4-Ph-U possibilities. This de novo design exercise with HIV-RT as the target resulted in identification of Het = 2-thiazolyl and U = dimethylallyloxy as a promising pair. Subsequent synthesis of the thiazole **1** in Figure 1.3 did provide a 10-μM lead in an MT-2 cell-based assay for anti-HIV activity. As described below, the lead was optimized to multiple highly potent NNRTIs, including the chlorotriazine in Figure 1.2 (31 nM), the corresponding chloropyrimidine (10 nM), and the cyanopyrimidine analog **2** (2 nM).[11–14]

Some additional details should be noted. The host, typically a protein, is rigid in the BOMB optimizations except for variation of terminal dihedral angles for side chains with

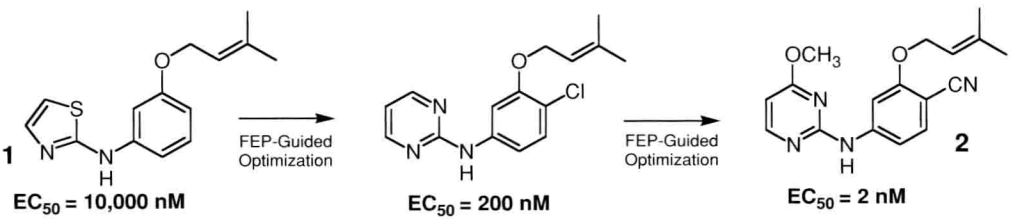

Figure 1.3. Example of a 10-μM lead proposed by BOMB that was optimized to provide numerous potent anti-HIV agents.

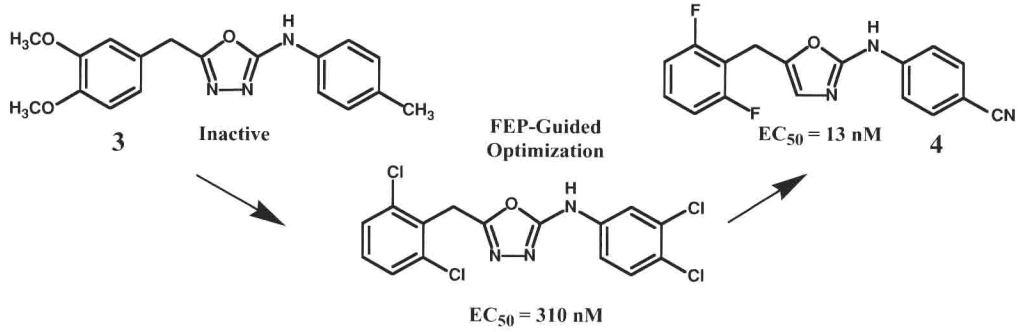

Figure 1.4. Progression of a false positive from docking to potent anti-HIV agents.

hydrogen-bonding groups, for example, the OH of tyrosine or serine and ammonium group of lysine. The current scoring function has been trained to reproduce experimental activity data for more than 300 complexes of HIV-RT, COX-2, FK506 binding protein, and p38 kinase.[5] It yields a correlation coefficient r^2 of 0.58 for the computed versus observed log(activities). The scoring function contains only five descriptors that were obtained by linear regression, including an estimate of the analog's octanol/water partition coefficient from QikProp (QPlog*P*),[15] the amount of hydrophobic surface area for the protein that is buried on complex formation, and an index recording mismatched protein/analog contacts, such as a hydroxyl group in contact with a methyl group. Interestingly, the most significant descriptor is QPlog*P*, which alone yields a fit with an r^2 of 0.47. Thus, the adage that increased hydrophobicity leads to increased binding is well supported, though it requires refinement for quality of fit using the host/ligand interaction energy or an index of mismatched contacts. Overdone, it also leads to ADME problems, especially poor aqueous solubility and high serum protein binding.

The results from a BOMB run include the structure for each protein/analog complex as a Protein Data Bank (PDB) file or BOSS/MCPRO Z-matrix (internal coordinate representation)[16] and a spreadsheet with one row for each analog summarizing computed quantities from the BOMB calculations, including host–analog energy components and surface area changes as well as predicted properties for the analog, including log $P_{o/w}$, aqueous solubility, and Caco-2 cell permeability from QikProp, which is called as a subroutine. The processing time for Het-NH-Ph-U using ammonia as the core is approximately 15 s per analog on a 3-GHz Pentium IV processor. The required time increases roughly linearly with the number of conformers that need to be constructed. For large libraries, multiple processors are used.

Virtual screening

The common alternative is to perform virtual screening on available compound collections using docking software. Many reviews and comparisons for alternative software and scoring functions are available.[6,17–20] There is no question that there have been many successes with docking such that, given a target structure, it is expected to be competitive with and far more cost effective than HTS and is now an important component of lead discovery programs in the pharmaceutical industry. New success stories are reported regularly in the literature and at conferences. However, it is generally accepted that correct rank-ordering of compounds for activity is beyond the current capabilities. This is not surprising in view of the thermodynamic complexity of host/ligand binding, including potential structural changes for the host on binding, which have usually been ignored, and the need for careful consideration of changes in conformational free energetics between the bound and unbound states.[21]

In our experience, docking has been a valuable complement to de novo design (Figure 1.1). When large compound collections are docked, interesting structural motifs often emerge as potential cores that may have been overlooked otherwise. Our earliest docking effort started out well, was formally a failure, and then recovered to provide an interesting lead series that yielded potent anti-HIV agents.[5,22] Leads were sought by processing a collection of approximately 70,000 compounds from the Maybridge catalog, which was supplemented with twenty known NNRTIs. The screening protocol began with a similarity filter that retrieves 60% of the known actives in the top 5% of the screened library. The approximately 2,000 library compounds that were most similar to the known actives were then docked into the 1rt4 structure of wild-type HIV-RT, using Glide 3.5 with standard precision.[6] The top 500 compounds were then redocked and scored in Glide extraprecision (XP) mode.[23] The top 100 of these were postscored with a molecular mechanics/generalized Born/surface area (MM-GB/SA) method that was shown to provide high correlation between predicted and observed activities for NNRTIs.[22] Though known NNRTIs were retrieved well (ten were ranked in the top twenty), purchase and assaying of approximately twenty high-scoring compounds from the library failed to yield any active anti-HIV agents. Persisting, the highest-ranked library compound, the inactive oxadiazoles **3** in Figure 1.4, was pursued computationally to seek

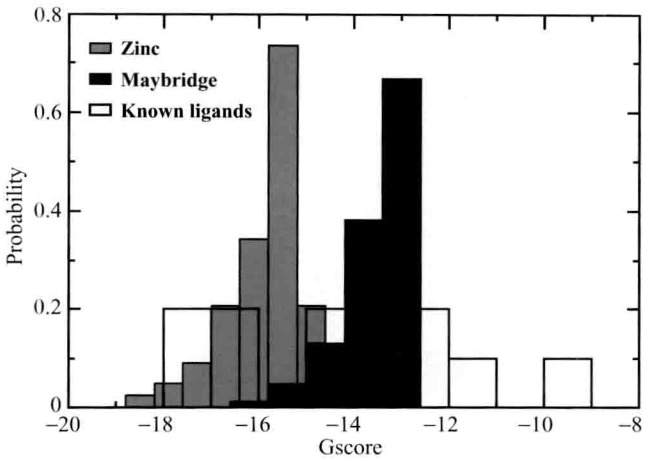

Figure 1.5. Distributions of the Glide XP scores for the top-ranked 1,000 ZINC compounds, the top-ranked 1,000 Maybridge compounds, and the 10 known tautomerase inhibitors.

constructive modifications. Specifically, the substituents were removed to yield the anilinylbenzyloxadiazole core. A set of small substituents was reintroduced in place of each hydrogen using BOMB; scoring with BOMB, followed by free-energy perturbation (FEP)-guided optimization, led to synthesis and assaying of several polychloro analogs with EC_{50} values as low as 310 nM in the MT-2 HIV-infected T-cell assay.[5] Further cycles of FEP-guided optimization led to novel, very potent NNRTIs, including the oxazole derivative **4**, as described more below.[24]

A more recent virtual screening exercise was strikingly successful.[25] New protocols had evolved, including use of the much larger ZINC database of approximately 2.1 million commercially available compounds.[26] The goal in this case was to disrupt the binding of macrophage migration inhibitory factor (MIF) to its receptor CD74, an integral membrane protein, and a major histocompatibility complex (MHC) class II chaperone. MIF is a pro-inflammatory cytokine that is released by T-cells and macrophages. It plays a key role in a wide range of inflammatory diseases and is involved in cell proliferation and differentiation and angiogenesis.[27,28] Curiously, MIF is also a keto-enol isomerase. There is evidence that the interaction of MIF with CD74 occurs in the vicinity of the tautomerase active site and that MIF inhibition is directly competitive with MIF/CD74 binding.[29] The docking was performed using GLIDE 4.0 and the 1ca7 crystal structure of the complex of MIF with *p*-hydroxyphenylpyruvate.[30] In addition to the ZINC collection, the Maybridge HitFinder library was screened, which provided an additional 24,000 compounds. After all structures were processed using SP GLIDE, the top-ranked 40,000 from ZINC and 1,000 from Maybridge were redocked and rescored using GLIDE in XP mode.[23] GLIDE XP scoring was also shown to provide good correlation with experimental data for 10 known inhibitors of MIF's tautomerase activity.

A key observation from the docking is illustrated in Figure 1.5, which shows the distributions of GLIDE XP scores for the top-ranked 1,000 compounds from ZINC, the top-ranked 1,000 Maybridge compounds, and the ten known MIF inhibitors. Clearly, the large ZINC collection yields many compounds with much more promising XP scores than the Maybridge HitFinder library. The average molecular weights for the two sets of 1,000 compounds are 322 for ZINC and 306 for Maybridge. The variation only amounts to one additional nonhydrogen atom for the ZINC set, so the improved performance with the ZINC collection presumably results from greater structural variety. In view of the sensitivity of activity to structure, as reflected in Figures 1.3 and 1.4, it is highly unlikely that active compounds can be found in small libraries like Maybridge HitFinder unless the assays can be run with the compounds at millimolar or higher concentrations, which is often precluded by solubility limits. Even with a viable core (Figure 1.4), the chance is low that a small library will contain a derivative with a substituent pattern that yields an active in a typical assay.

Finally, the GLIDE poses for approximately 1,200 of the top-ranked compounds were displayed and 34 compounds were selected by human evaluation of the poses with input from QIKPROP on predicted properties and structural liabilities. The filtering included rejection of poses where the conformation of the ligand was energetically unlikely or where there were overly short intramolecular contacts and compounds with generally undesirable features such as readily hydrolizable functional groups or substructures such as coumarins, which are promiscuous protein binders. Only 24 of the 34 selected compounds were, in fact, available for purchase, which represents a typical ratio. Ultimately 23 compounds were submitted to a protein-protein binding assay using immobilized CD74 and biotinylated human MIF with streptavidin-conjugated alkaline phosphatase processing *p*-nitrophenyl phosphate as substrate. Remarkably, eleven of the compounds were found to have inhibitory activity in the μM regime including four compounds with IC_{50} values below 5 μM. Inhibition of MIF tautomerase activity was also established for several of the compounds with IC_{50} values as low as 0.5 μM. Representative active compounds are shown in Figure 1.6; optimization of several of the lead series is being pursued. Notably, these are the most potent small-molecule inhibitors of MIF-CD74 binding that have been reported to date.

The first three compounds in Figure 1.6 were ranked in 285th, 696th, and 394th place by the XP scoring, so they were not "high in the deck." However, prior de novo structure building with BOMB had indicated that 6–5 fused bicyclic cores should be promising, so the selections were biased in this direction. The compound ranked first with XP GLIDE was also purchased and assayed; it turned out to be the 250-μM inhibitor in Figure 1.6. In addition, the compounds ranked 26th and 32nd were purchased and found to be inactive. Overall, it is expected that contributors to the success with the virtual screening in this case were

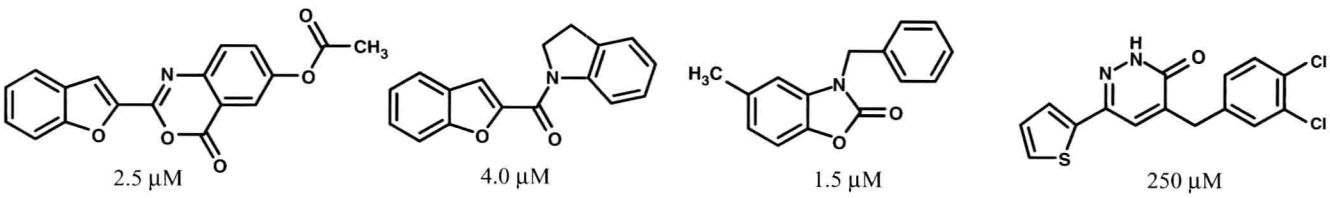

Figure 1.6. Structures and IC_{50} values for some inhibitors of MIF-CD74 binding discovered by virtual screening.

improvements with GLIDE 4.0 and the XP scoring, use of the large ZINC library, the relatively small binding site and consequently small number of rotatable bonds for potential inhibitors, and the human filtering.

ADME ANALYSES

As indicated in Figure 1.1, as one pursues leads it is important to be aware of potential pharmacological liabilities. The significance of this issue became increasingly apparent in the 1990s because of high failure rates for compounds in clinical trials that could be ascribed to ADME and toxicity problems.[31] This led to the introduction of Lipinski's rules and recognition that compounds developed in the post-HTS era frequently tended to be too large and hydrophobic, which is accompanied by solubility and bioavailability deficiencies.[32] In this atmosphere, more effort was placed on quantitative prediction of molecular properties beyond log $P_{o/w}$ using statistical procedures such as regression analyses and neural networks, which were trained on experimental data.[33,34] The typical regression equation is a linear one, Equation (1.1), where the sum is over molecular descriptors i that have values c_i for the given structure and the coefficients a_i are determined to minimize the error with the experimental data:

$$property = \sum_i a_i c_i + a_0. \tag{1.1}$$

In Figure 1.1, the choice for ADME analyses is QIKPROP, which was among the earliest programs to predict a substantial array of pharmacologically relevant properties. Version 1.0, which was released in March 2000, provided predictions for intrinsic aqueous solubility, Caco-2 cell permeability, and hexadecane/gas, octanol/gas, water/gas, and octanol/water partition coefficients. The required input for QIKPROP is a three-dimensional structure of an organic molecule, and it mostly uses linear regression equations with molecular descriptors such as surface areas and hydrogen-bond donor and acceptor counts. By version 3.0 from 2006, the output covered eighteen quantities, including log BB for brain/blood partitioning, log K_{hsa} for serum albumin binding, hERG K^+ channel blockage, primary metabolites, and overall percentage human oral absorption.[15] The prediction of primary metabolites is based on literature precedents and recognition of corresponding substructures; for example, methyl ethers and tolyl methyl groups are typically metabolized to the alcohols. Execution time with QIKPROP is negligible because the most time-consuming computation is for the molecule's surface area. Average root-mean-square (rms) errors for most quantities are about 0.6 log unit, as in Figure 1.7.

To gauge acceptable ranges of predicted properties, QIKPROP 3.0 was used to process approximately 1,700 known neutral oral drugs,[13] which were compiled by Proudfoot.[35] For submission to QIKPROP, the original two-dimensional structures were converted to three-dimensional structures and energy-minimized with BOSS using the OPLS/CM1A force field.[10,16] Some key results from the analyses are summarized as histograms in Figures 1.8 and 1.9. Consistent with the log $P_{o/w}$ limit of 5 in Lipinski's rules,[32] 91% of oral drugs are found to have

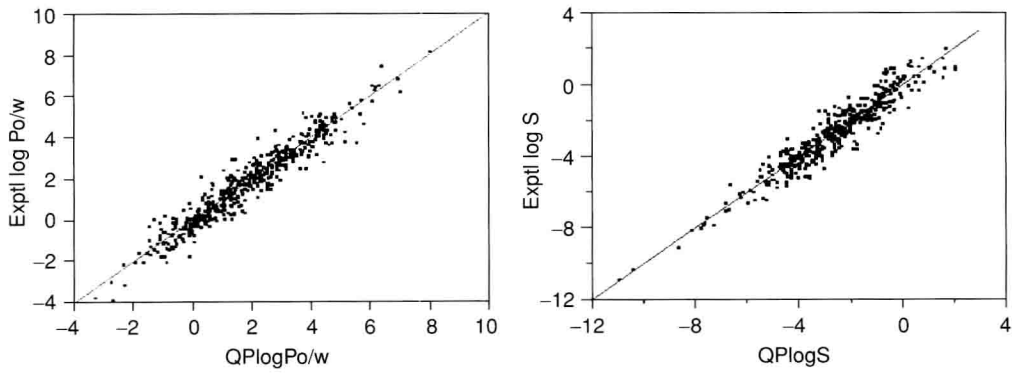

Figure 1.7. Experimental data and QikProp 3.0 results for 400–500 octanol/water partition coefficients (left) and aqueous solubilities (right). S is aqueous solubility in moles per liter. Correlation coefficients r^2 are 0.92 and 0.90 and the rms errors are 0.54 and 0.63 log unit, respectively.

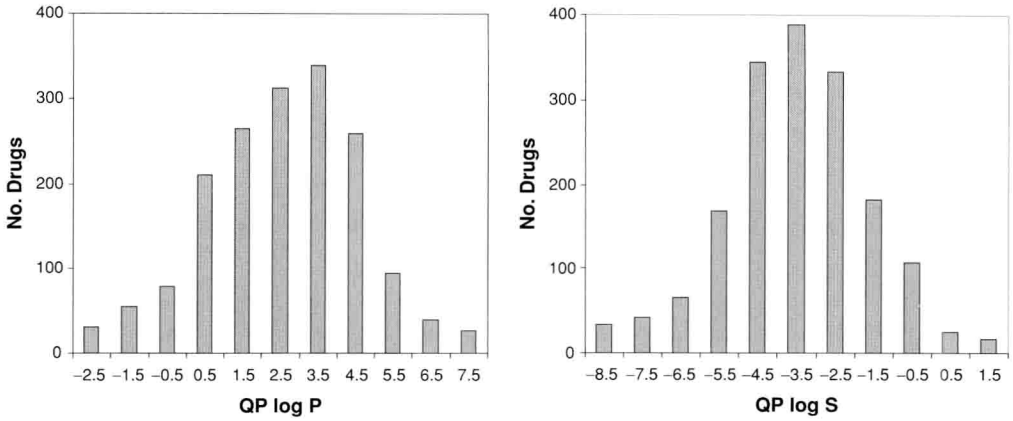

Figure 1.8. QikProp distributions for log $P_{o/w}$ (left) and log S (right) for 1712 oral drugs.

QPlog*P* values below 5.0. However, values below zero are uncommon, presumably because of poor cell permeability, and the "sweet" range for log $P_{o/w}$ appears to be 1–5. For aqueous solubility, 90% of the QPlog*S* values are above −5.7, that is, *S* is greater than 1 μM. QPlogS values less than −6 or greater than −1 are undesirable. The QikProp results also state that 90% of oral drugs have cell permeabilities, P_{Caco}, above 22 nm/s and no more than six primary metabolites. These quantities and limits address important components of bioavailablility, namely, solubility, cell permeability, and metabolism.

For our design purposes (Figure 1.1), a compound is viewed as potentially ADME challenged if it does not satisfy all components of a "rule-of-three": predicted log $S > -6$, $P_{Caco} > 30$ nm/s, and maximum number of primary metabolites of 6. For central nervous system (CNS) activity requiring blood-brain barrier penetration, an addendum is that QPlogBB should be positive. Also, some caution is warranted for a compound with no metabolites because of possible clearance problems.[17] A further note is that QPlog*P* and QPlog*S* are correlated with an r^2 of 0.68, so there would be some redundancy in invoking limits on both. Among reasons for preferring solubility, there are quite a few examples of relatively small drugs that have log $P_{o/w}$ values greater than 5 but have acceptable solubility, for example, meclizine, prozapine, clocinizine, bepridil, denaverine, bopindolol, phenoxybenzamine, and terbinafine. Of course, compounds with reactive functional groups, for example, those that are readily hydrolizable or strongly electrophilic, are flagged by QikProp and normally eliminated from inclusion in a lead structure. For example, in rofecoxib (Vioxx) concern could be expressed for possible nucleophilic attack and ring opening at the furanone carbonyl and for Michael addition to the α,β-double bond; metabolic oxidation at the allylic methylene group is also expected to yield the 5-hydroxy derivative (Scheme 1). For celecoxib (Celebrex), metabolic oxidation to the benzylic alcohol is noted by QikProp, and an "alert" is given that

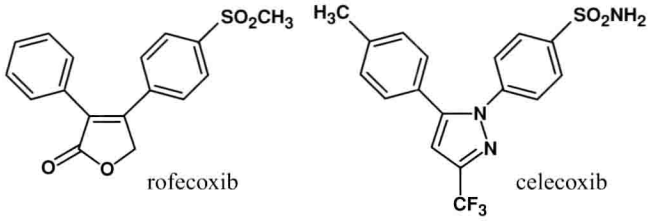

Scheme 1.

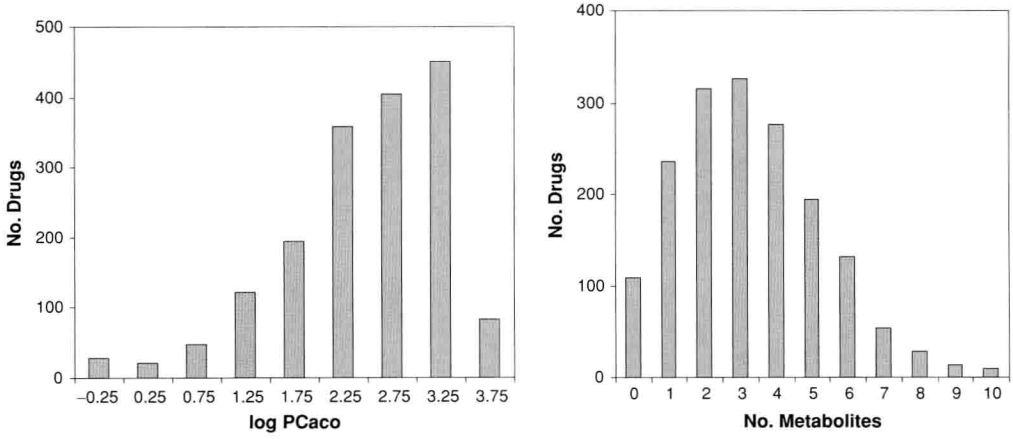

Figure 1.9. QikProp distributions for log P_{Caco} (left) and number of primary metabolites (right) for 1,712 oral drugs. P_{Caco} is the Caco-2 cell permeability in nm/s.

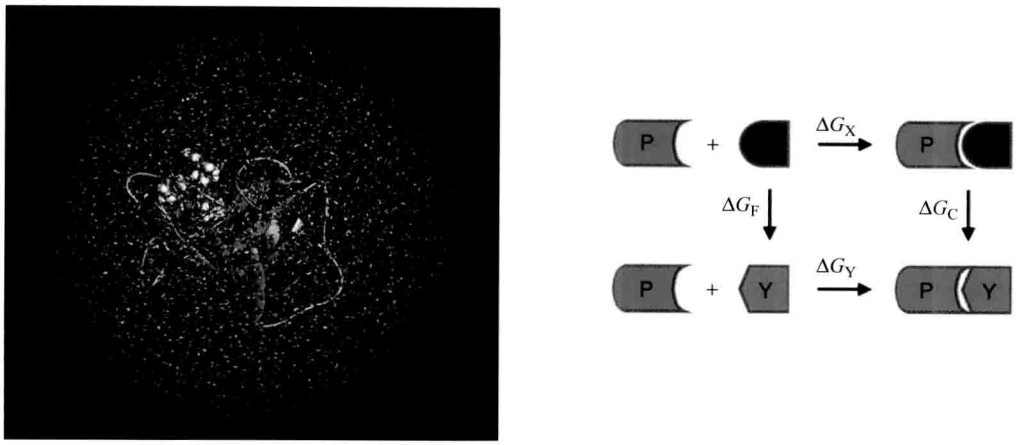

Figure 1.10. (Left) A protein/ligand complex surrounded by approximately 1,000 water molecules in a spherical shell or "cap." (Right) Thermodynamic cycle used to compute relative free energies of binding, $\Delta\Delta G_b$. P is a host and X and Y are two ligands.

the primary sulfonamide group can be associated with sulfa allergies and indiscriminant metal chelation.[36]

Overall, for the 1,712 oral drugs, 278 violate one or more of the four Lipinski rules (MW $<$ 500, $\log P_{o/w} < 5$, H-bond donors $\leq$ 5, H-bond acceptors $\leq$10) with QPlog$P$ used for log $P_{o/w}$. There are 178, 82, and 18 oral drugs with one, two, and three violations, respectively. The group with two violations includes macrolides such as erythromycin and azithromycin and some other well-known drugs like atorvastatin, amiodarone, chloramphenicol, ketoconazole, and telmisartan. These examples all fail one member of the rule-of-three, either the solubility limit or number of primary metabolites, for example, respectively, atorvastatin and the macrolides. The group with three rule-of-five violations includes the HIV-protease inhibitors ritonavir and saquinavir, which are known to have low bioavailability. There are exceptions to such rules because they are based on 90th-percentile limits. Nevertheless, in all stages of lead generation, it would be imprudent to ignore property distributions for known drugs such as those in Figures 1.8 and 1.9.

LEAD OPTIMIZATION

It is assumed that inhibitory potency increases with increasing biomolecule-inhibitor binding. So, on the computational side, the key for lead optimization is accurate prediction of biomolecule-ligand binding affinities. There are many approaches, but the potentially most accurate ones are the most rigorous.[17] At this time, the best that is done is to model the complexes in the presence of hundreds or thousands of explicit water molecules using Monte Carlo (MC) statistical mechanics or molecular dynamics methods (Figure 1.10).[17] Classical force fields[16] are used, and extensive sampling is performed for key external (translation and rotation) and internal degrees of freedom for the complexes, solvent, and any counterions. FEP and thermodynamic integration (TI) calculations then provide formally rigorous means to compute free-energy changes.[37] For biomolecule/ligand affinities, perturbations are made to convert one ligand to another using the thermodynamic cycle in Figure 1.10. The conversions involve a coupling parameter, λ, that causes one molecule to be smoothly mutated to the other by changing the force field parameters and geometry.[38] The difference in free energies of binding for the ligands X and Y then comes from $\Delta\Delta G_b = \Delta G_X - \Delta G_Y = \Delta G_F - \Delta G_C$. Two series of mutations are performed to convert X to Y unbound in water and complexed to the biomolecule, which yield ΔG_F and ΔG_C.

Absolute free energies of binding are not obtained, but for lead optimization it is sufficient to assess the effects of making changes or additions to a core structure in the same spirit as synthetic modifications. Though the MC or MD plus FEP or TI calculations are rigorous, the accuracy of the results is affected by many issues, including the use and quality of force fields; missing energy terms, such as instantaneous polarization effects; and possible inadequate configurational sampling, which may be associated with, for example, infrequent conformational changes that are beyond the duration of the simulations. In the author's experience, more approximate methods are not accurate enough to provide satisfactory guidance in lead optimization.

The idea of using such calculations for molecular design goes back more than twenty years, at least to the report of the first FEP calculation for conversion of a molecule X to molecule Y in 1985[38] and to the earliest application of FEP calculations for protein-ligand binding by Wong and McCammon.[39] A final comment from McCammon's review on computer-aided molecular design in *Science* in 1987 was perspicacious: "The attentive reader will have noticed that no molecules were actually designed in the work described here."[40] The situation has remained basically unchanged since the late 1980s. As the convergence of FEP calculations was investigated, it was apparent that they were too computationally intensive for routine use in molecular

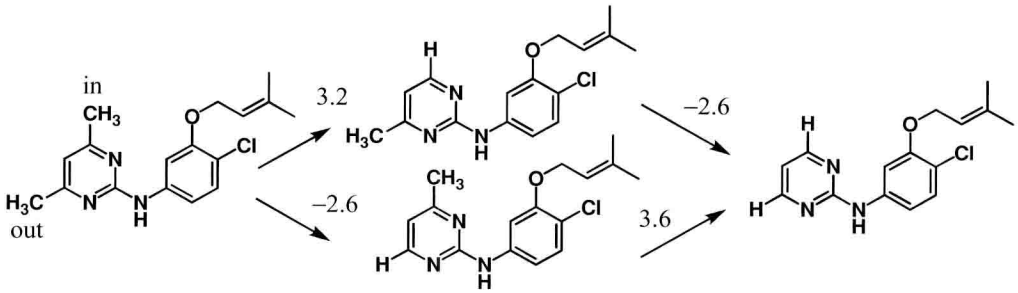

Figure 1.11. MC/FEP results for $\Delta\,\Delta G_b$ (kcal/mol) established a strong preference for a single methyl group oriented "in" toward Tyr188 in the NNRTI binding site. The precision of the calculations is reflected in the cycle's small hysteresis, 0.4 kcal/mol.

design given the computer resources available before ca. 2000. In 1985, the ethane-to-methanol FEP calculation in a periodic cube with 125 water molecules required two weeks on a Harris-80 minicomputer,[38] and the Wong/McCammon MD simulation for the trypsin-benzamidine complex covered only 29 ps but was performed on a Cyber 205 "supercomputer."[39]

Thus, until recently the application of FEP or TI calculations on protein-ligand systems predominantly featured retrospective calculations to reproduce known experimental inhibition data and generally addressed small numbers of compounds. Kollman was a strong advocate of the potential of free-energy calculations for molecular design, and he and Merz reported a rare, prospective FEP result on the binding of a phosphonamidate versus phospinate inhibitor with thermolysin.[41,42] Pearlman also advanced the technology, though publications in 2001 and 2005 were still retrospective and confined to a simple congeneric series of 16 p38 kinase inhibitors.[43,44] In addition, Reddy and Erion have been steady contributors; they have used FEP calculations to evaluate contributions of heteroatoms and small groups to the binding of inhibitors to gain insights on directions for improvement.[45,46] Our own computations on protein/ligand binding began to appear in 1997 using MC/FEP methodology.[47,48] Many issues and systems were subsequently addressed, including substituent optimization for celecoxib analogs,[49] COX-2/COX-1 selectivity,[50] and heterocycle optimization for inhibitors of fatty acid amide hydrolase.[51] An additional series of publications used MC/FEP calculations to compute the effects of HIV-RT mutations on the activity of NNRTIs.[52–55] The latter work included predictions for the structures of the complexes of efavirenz and etravirine with HIV-RT, which were subsequently confirmed by x-ray crystallography.[52,54,56] Confidence in the predicted structures came from agreement between the FEP results and experimental activity data.

FEP-guided optimization of azines as NNRTIs

With this preparation, large increases in computer resources, the hiring of synthetic chemists, and collaboration with biologists, FEP-guided lead optimization projects were initiated in 2004. Early successes in the optimization of potent NNRTIs are reflected in Figures 1.2 and 1.3 for the Het-NH-3-Ph-U series.[11–13] MC/FEP calculations were used to optimize the heterocycle and the substituent in the 4-position of the phenyl ring. The calculations are run with MCPRO and all use the OPLS/CM1A force field for the ligands and OPLS-AA for the protein.[10,16] This quickly led to selection of 2-pyrimidinyl and 2-(1,3,5)-triazinyl for the heterocycle and chlorine or a cyano group at the 4-position. These combinations yielded NNRTIs with EC_{50} values near 200 nM.

Extensive FEP calculations then focused on optimization of substituents for the heterocycle.[13] For the 2-pyrimidines, the immediate question concerned whether 4,6-disubstitution would be favorable or if mono substitution at the 4- or 6-position is preferred. In complexes with HIV-RT, the 4- and 6-positions are not equivalent; for example, in Figure 1.2, the methoxy group could be directed toward the viewer ("out") or away ("in"), as shown. From display of structures of the complexes, the preferences for in or out were not obvious. This was clarified by MC/FEP results, which showed a strong preference for having a single small substituent on the pyrimidine ring and that the substituent would be oriented "in" (Figure 1.11). Synthesis of a variety of such mono-substituted pyrimidines and triazines yielded ten NNRTIS with EC_{50}s below 20 nM.[11–13] There was good correlation between the FEP results and the observed activities.[11,13] The methoxypyrimidine **2** in Figure 1.3 (2 nM) was the most potent, although it was also relatively cytotoxic (CC_{50} = 230 nM). The corresponding 1,3,5-triazine is also a potent anti-HIV agent (11 nM) and has a large safety margin (CC_{50} = 42 μM).

Heterocycle scans

FEP results also established the orientation of the methoxy methyl group in the pyrimidine and triazine derivatives shown in Figure 1.2, that is, pointing toward Phe227 rather than Tyr181. This suggested the possibility of cyclizing the methoxy group back into the azine ring to form 6–5 and 6–6 fused heterocycles in the manner indicated in Scheme 2.